SUPPLEMENT

RESONANT ROSSBY WAVE TRIADS AND THE SWINGING SPRING

BY PETER LYNCH

ABSTRACT (From page xxxx)

The wave solutions discovered by Rossby are of fundamental importance for atmospheric dynamics. The nonlinear interactions between these waves determine the primary characteristics of the energy spectrum. These interactions take place between triplets of waves known as "resonant triads" and, for small amplitude, they are described by the three-wave equations. These same equations also govern the dynamics of a simple mechanical system, the elastic pendulum or *swinging spring*. This equivalence allows us to deduce properties, not otherwise evident, of resonant triads from the behavior of the mechanical system. In particular, the characteristic stepwise precession of the swing plane, so obvious from observation of the physical spring pendulum, is also found for the Rossby triads. This phenomenon has not been previously noted and is an example of the insight coming from the mathematical equivalence of the two systems. The implications of the precession for predictability of atmospheric motions are considered. The pattern of breakdown of unstable Rossby waves is very sensitive to unobservable details of the perturbations, making accurate prediction very difficult.

Rossby waves are solutions of simplified forms of the equations governing the dynamics of the atmosphere and oceans. They serve as archetypes for the sinuous large-scale motions of the midlatitude troposphere. They are horizontal transverse waves with large values of vorticity and with divergence that is negligible by comparison. Their most characteristic feature is that they move westward relative to the zonal atmospheric flow. This strange lopsidedness, or chirality, is a result of the earth's rotation, which breaks the symmetry of east–west reflection. The Rossby wave was the topic chosen by Professor George Platzman for his Symons Memorial Lecture to the Royal Meteorological Society, and an expository review has appeared (Platzman 1968). Several interesting articles on Rossby have appeared recently in *BAMS:* in particular, see Phillips (1998) and Lewis (1992). The dynamics of Rossby waves are discussed in considerable depth in Pedlosky (1987).

The atmospheric flow in middle latitudes is highly complex, and it is dominated by baroclinic instability. This results from the horizontal temperature gradient arising from differential insolation, and from the vertical wind shear, which is associated with it

AFFILIATION: LYNCH—Met Éireann, Dublin, Ireland
CORRESPONDING AUTHOR: Peter Lynch, Met Éireann, Glasnevin Hill, Dublin 9, Ireland
E-mail peter.lynch@met.ie
DOI: 10.1175/BAMS-84-5-Lynch

In final form 3 December 2002
©2003 American Meteorological Society

through geostrophic balance and the thermal wind relationship. However, to a first approximation, the middle-latitude flow may be described as an axially symmetric circumpolar cyclonic vortex with superimposed wave perturbations (Charney 1973). In simple terms, it is a westerly zonal flow upon which large horizontal waves are superimposed. We can regard these waves as physical manifestations of the idealized Rossby waves.

FIG. S1. Jule Charney (1917–81), from the cover of *Eos*, 57, Aug 1976 (copyright Nora Rosenbaum).

The full equations governing atmospheric dynamics are overly complicated and include, in addition to the meteorologically significant motions, physical phenomena that have little import on the weather. Thus, the full spectrum of sound waves is embraced within the set of solutions. Gravity waves are another class of solutions of the full system, which, for many purposes, can be regarded as a noisy nuisance. One of the key advances enabling the application of quantitative methods to weather forecasting was the development of simplified systems of equations, from which irrelevant or unimportant solutions were eliminated or filtered out. And one of the outstanding contributions to this development was the seminal paper of Charney (1948).

Charney (Fig. S1) introduced scale analysis to examine and compare the relative sizes of the various terms in the equations of motion. He recognized that the dominant motion is approximately hydrostatic, geostrophic, adiabatic, and horizontal; that the gravity waves are of secondary importance; and that only the vortical waves—the rotational waves with large vorticity and small divergence—are of importance for modeling and prediction of large-scale weather phenomena. By elimination of divergence and systematic use of the geostrophic relationship, he reduced the system to a single equation for a single variable, the *potential vorticity*. The conservation of quasigeostrophic potential vorticity is the fundamental principle governing large-scale atmospheric dynamics. The historical development of quasigeostrophic theory has been described by Phillips (1990). For biographical information on Charney, and his most important publications, see Lindzen et al. (1990).

The simplest context for the study of Rossby waves is a shallow layer of incompressible fluid on a rotating earth. The geometry is greatly simplified by ignoring the effects of sphericity except in one crucial respect: we allow for the change in the vertical component of the earth's rotation with latitude. This is called the beta-plane approximation; it was introduced by Rossby in his ground-breaking paper of 1939 in which the Rossby wave formula first appeared. In fact, Rossby's discovery was adumbrated more than half a century earlier: the solutions of the Laplace tidal equations (the linearized shallow water equations on a sphere) had been discussed by Margules (1893) and by Hough (1898), both of whom had identified two different classes of solutions. Lamb (1895) had also considered solutions of this system in the second edition of his *Hydrodynamics*. Also, Haurwitz (1937) had come tantalizingly close to identifying the crucial elements of the dynamics of the rotational waves (Platzman 1985). However, it was Rossby who had the intuitive genius to isolate the factors that were essential for the existence of these waves, and to elucidate their dynamics by studying them in a model of maximum simplicity.

Almost immediately after the appearance of Rossby's paper, Haurwitz generalized the solutions to allow for finite lateral extent (Haurwitz 1940a) and for spherical geometry (Haurwitz 1940b), and related them to Margules's oscillations of the second class. To take full account of divergence, the Laplace tidal equations, the linearized shallow water equations on a sphere, must be considered. The eigenfunctions of these equations are called Hough functions, and they fall into two distinct categories, gravity waves and rotational waves. They have been comprehensively described by Longuet-Higgins (1968), Flattery (1967), and Kasahara (1976). A fuller discussion of the development of Rossby wave theory is presented in Platzman's (1968) Symons Lecture (loc. cit.), and also in a recent scientific history of tides (Cartwright 1999).

CONSERVATION OF POTENTIAL VORTICITY. We shall consider a shallow layer of incompressible fluid on a rotating planet. With the beta-plane approximation, we can use rectangular coordinates x and y. Under the assumptions of quasigeostrophic theory, the dynamics reduce to a single

equation expressing the conservation of potential vorticity. This appears in Charney's (1948) paper as his Eq. (56). We shall follow the notation of Pedlosky and write it in the form

$$\frac{\partial}{\partial t}\left(\nabla^2\psi - F\psi\right) + \left(\frac{\partial\psi}{\partial x}\frac{\partial\nabla^2\psi}{\partial y} - \frac{\partial\psi}{\partial y}\frac{\partial\nabla^2\psi}{\partial x}\right) + \beta\frac{\partial\psi}{\partial x} = 0, \tag{1}$$

an equation for the streamfunction ψ. The parameter β is the variation with latitude of the Coriolis parameter f, twice the vertical component of the earth's rotation. The parameter F is equal to $1/L_R^2$ where $L_R = (gH_0)^{1/2}/f$ is called the Rossby radius of deformation, H_0 is the mean depth, and g is the acceleration due to gravity. The second expression in parentheses is the Jacobian $J(\psi,\nabla^2\psi)$, representing nonlinear advection of vorticity.

Equation (1) expresses the conservation, following the motion, of the barotropic quasigeostrophic potential vorticity. It may be written in the form

$$\left(\frac{\partial}{\partial t} + \boldsymbol{V}\cdot\nabla\right)q = 0,$$

where the velocity is given by $\boldsymbol{V} = \boldsymbol{k}\times\nabla\psi$ and the potential vorticity $q = \zeta - F\psi + f$ is a sum of three components. The first two are the relative vorticity $\zeta = \nabla^2\psi$ due to the fluid motion, and a contribution from variations in the free surface height (the streamfunction ψ is related to the depth h of the fluid by the simple relationship $f\psi = gh$). The third component is the planetary vorticity f, due to the earth's rotation. The variation of this ambient vorticity with latitude is β, the crucial factor for the existence of Rossby wave solutions. The relative importance of the first two terms in q depends on the ratio of the horizontal scale L of the motion to the Rossby radius L_R. The deformation radius is the scale for which the relative vorticity ζ and variations of surface height h make equal contributions to the potential vorticity. For $L \ll L_R$, the term involving F is negligible.

It is easy to find wavelike solutions of (1). We temporarily neglect the nonlinear Jacobian term, seek a solution of the form $\psi = A\cos(kx + \ell y - \sigma t)$, and find that it satisfies the equation provided that the frequency σ satisfies the dispersion relationship:

$$\sigma = -\frac{k\beta}{k^2 + \ell^2 + F}. \tag{2}$$

This is the celebrated Rossby wave formula.[1] A detailed discussion of these solutions is presented in Pedlosky (1987). We note only the consequence of the minus sign in (2): because the zonal phase speed $c = \sigma/k$ is negative, these waves always travel toward the west. As long as we neglect the nonlinear terms, we can superimpose a number of Rossby wave solutions with differing wavenumbers $K = (k,\ell)$ and frequencies σ. Each component will travel at a different rate, and each will evolve independently of its fellow travelers.

The Jacobian term vanishes for a single Rossby wave: the isolines of vorticity are parallel to the streamlines, so the gradient of vorticity is perpendicular to the velocity and the advection vanishes. This means that a pure Rossby wave is a solution of the full nonlinear equation (1). However, if more than one component is present, the velocity of one component advects the vorticity of another, and the components are no longer independent but interact through the nonlinear term in (1). Suppose we start with just two components. They will interact with each other to produce a third component, whose wavenumber and frequency are the sums of their wavenumbers and frequencies. This third component will in turn interact with the first two, producing further components. In this sense, a pure Rossby wave is an unstable solution of (1); inevitable small perturbations will have projections onto other components, and these will interact nonlinearly with the primary wave to produce still further components. Eventually, the solution will be transformed out of all recognition.

It is remarkable that Rossby waves have been "rediscovered" in a completely different physical context, that of instabilities in a magnetically confined plasma. Hasegawa and Mima (1977) investigated wave motions of an inhomogeneous plasma, and derived an equation that is mathematically identical to (1). Their wave solutions, called *drift waves,* are dynamically equivalent to Rossby waves. The quantity corresponding to the variation of the ambient vorticity in a fluid (the beta parameter) is the variation of the background plasma density. The correspondence between Rossby waves in the atmosphere and drift waves in plasmas has been thoroughly explored by Horton and Hasegawa (1994).

[1] In fact, Rossby ignored the y variations and assumed conservation of absolute vorticity $\zeta + f$, so the free surface height variation did not enter, and he obtained the simpler form of the dispersion relationship, $\sigma = -\beta/k$. He also allowed for a mean zonal velocity, $\overline{u}$, which Doppler shifts the wave solution.

When considering the meteorological origins of (1), plasma physicists have adopted the name *Charney's equation* (e.g., Horton and Hasegawa 1994) or the *Charney–Obukhov equation* (e.g., Nezlin and Snezhkin 1993). In the plasma context it is called the *Hasegawa–Mima equation* (Hasegawa and Mima 1977). Charney (1948) was the first to present a systematic derivation based on scale analysis and to clarify the precise conditions for its validity. Obukhov (1949) derived an equation of essentially the same form [he omitted the beta term in his analysis, but he was aware of its importance for planetary-scale motions; see Phillips et al. (1960)]. However, the equation was known before the publications of Charney and Obukhov, and was used by other workers, most notably by Rossby. Thus, we feel it inappropriate to follow the practice in plasma physics, so we will continue to refer to (1) by its "dynamical" title, the quasigeostrophic barotropic potential vorticity equation.

A more appropriate equation to bear Charney's name is the three-dimensional quasigeostrophic quasi-potential vorticity equation. This was first derived by Charney (1948), and presented later in a more elegant formulation by Charney and Stern (1962). It may be written

$$\left(\frac{\partial}{\partial t}+\frac{\partial\psi}{\partial x}\frac{\partial}{\partial y}-\frac{\partial\psi}{\partial y}\frac{\partial}{\partial x}\right)\times \left[\frac{\partial^2\psi}{\partial x^2}+\frac{\partial^2\psi}{\partial y^2}+\frac{1}{\rho_S}\frac{\partial}{\partial z}\left(\frac{\rho_S}{S}\frac{\partial\psi}{\partial z}\right)+\beta y\right]=0, \quad (3)$$

where $\rho_S(z)$ is the mean density and S the stability parameter. This is the form given in Pedlosky (1987, p. 358), where the notation is more fully defined. Eq. (1) is the barotropic limit of (3). Charney contributed substantially to our understanding of atmospheric dynamics by showing that for synoptic-scale three-dimensional motions, the vertical velocity, which enables the stretching of planetary vorticity filaments, can be eliminated by means of the thermodynamic equation, which leads to Eq. (3), a single equation for a single unknown, the quasigeostrophic potential vorticity.

RESONANT ROSSBY WAVE TRIADS. There is a case of special interest in which two wave components produce a third wave, such that its interaction with each of them generates the other. In this case, the nonlinear interaction is essentially confined to three components that exchange energy but do not produce any further waves. These three waves are called a *resonant triad.* The form of the solution is

$$\Psi=\sum_{n=1}^{3}\Re\left\{a_n(t)\exp\left[i\left(k_n x+\ell_n y-\sigma_n t\right)\right]\right\}, \quad (4)$$

where the amplitudes $a_n = |a_n(t)|\exp[i\varphi_n(t)]$ are time dependent, and σ_n is related to (k_n, ℓ_n) through (2). But not just any three waves will do; they must satisfy restrictive conditions on their wavenumbers and frequencies. The wavenumbers $K_n = (k_n, \ell_n)$ must sum to zero, so must the frequencies σ_n. This guarantees that each pair of components interacts nonlinearly to produce a total phase $kx + \ell y - \sigma t$, corresponding to that of the third component and that strong interaction between the waves occurs.

To study the dynamics of Rossby wave triads, Pedlosky (1987) used a two-timing perturbation approach, assuming that the envelope amplitudes $a_n(t)$ vary slowly compared to variations due to the movements of the waves. We shall eschew mathematical details, referring the interested reader to that excellent text for a full exposition, and just set down the main results.[2] The Rossby wave combination (4) satisfies the complicated *partial* differential equation (1). The three amplitudes of a resonant triad satisfy a drastically simplified system of three *ordinary* differential equations

$$\begin{aligned}\kappa_1^2\dot{a}_1+B_1a_2^*a_3&=0,\\ \kappa_2^2\dot{a}_2+B_2a_3a_1^*&=0,\\ \kappa_3^2\dot{a}_3+B_3a_1a_2&=0,\end{aligned} \quad (5)$$

where dots denote time derivatives and asterisks denote complex conjugates. The coefficients for the tendencies are $\kappa_n^2 = K_n^2 + F$, where $K_n^2 = k_n^2 + \ell_n^2$, and the interaction coefficients are $B_1 = \frac{1}{2}(k_2\ell_3 - k_3\ell_2)(K_2^2 - K_3^2)$, with B_2 and B_3 defined by cyclic permutation of indices. It follows that $B_1 + B_2 + B_3 = 0$, so that two of these are positive and one negative, or vice versa. With periodic boundary conditions, the solutions of the barotropic potential vorticity equation (1) conserve not only the total energy, but also the potential enstrophy, the square of the relative potential vorticity. These conservation properties have a special significance for a wave triad. They are expressed as

[2] Pedlosky neglected variations in φ_n, but we shall find them to be of interest. The complex forms of the three-wave equations were considered by Bretherton (1964).

$$E = \tfrac{1}{4}(\kappa_1^2 a_1^2 + \kappa_2^2 a_2^2 + \kappa_3^2 a_3^2), \quad (6)$$

$$S = \tfrac{1}{4}(\kappa_1^4 a_1^2 + \kappa_2^4 a_2^2 + \kappa_3^4 a_3^2). \quad (7)$$

We shall see that the conservation of E and S has a profound influence on the character of the flow.

We assume that the wave components are ordered so that $K_1 < K_3 < K_2$. That is, the *third* component has an *intermediate* horizontal scale. This is consistent with arrangement in order of increasing frequency, so that $|\sigma_1| < |\sigma_2| < |\sigma_3|$ (Pedlosky 1987, p. 176). Then, defining

$$A_n = \mu_1\mu_2\mu_3\left(\frac{a_n}{\mu_n}\right), \quad n = 1,2,3, \quad (8)$$

where $\mu_n^2 = |B_n/\kappa_n^2|$, the modulation equations, that is, the equations for the envelope amplitudes, may be written as

$$\begin{aligned} \dot{A}_1 &= -A_2^* A_3, \\ \dot{A}_2 &= -A_3 A_1^*, \\ \dot{A}_3 &= +A_1 A_2. \end{aligned} \quad (9)$$

This is the canonical form of the *three-wave equations.* They are the canonical equations resulting from the Hamiltonian $H = \Im(A_1 A_2 A_3^*)$, which is a constant of the motion (Holm and Lynch 2002). The energy and enstrophy may be linearly combined to give two constants known as the Manley–Rowe quantities:

$$N_1 = |A_1|^2 + |A_3|^2, \; N_2 = |A_2|^2 + |A_3|^2. \quad (10)$$

This is remarkable: if the energy of the wave with an intermediate scale (the third component) grows, both the smaller and larger waves must lose energy. Similarly, the largest and smallest components grow together at the expense of the intermediate one. Because $J = N_1 - N_2 = |A_1|^2 - |A_2|^2$ is constant, the squares of the amplitudes $|A_1|$ and $|A_2|$ rise and fall together by equal amounts. Thus, it is impossible for energy to be transferred only to larger or to smaller scales. These conditions put strong constraints on the distribution of energy in the atmosphere and are the primary reason why there is a preponderance of energy at large scales.

Equations (9) are nonlinear, but completely integrable. The Manley–Rowe relations allow elimination of two of the amplitudes, yielding a single equation for the third. Full analytical solutions can be expressed in terms of Jacobi elliptic functions (Bretherton 1964; Lynch 2002a). However, we are more concerned with qualitative features of the solutions than with quantitative detail. Some insight is provided by a particular solution in terms of elementary functions. It is easily shown by direct substitution that

$$A_1 = A_2 = \gamma \operatorname{sech} \gamma(t - t_0), \; A_3 = \gamma \tanh \gamma(t - t_0), \quad (11)$$

satisfies (9) for arbitrary γ and t_0. This solution is the so-called *homoclinic orbit.* The trajectory in phase space emanates from the homoclinic point, corresponding to an unstable equilibrium, and returns there after infinite time. The conserved quantities for this solution have the values $H = J = 0$ and $N_1 = N_2 = \gamma^2$. The amplitudes of the wave components are in the ratio $a_1{:}a_2{:}a_3 = \mu_1{:}\mu_2{:}\mu_3 \sinh \gamma t$. For large negative time, wave 3 dominates. It gradually decreases in energy as waves 1 and 2 grow until time $t = t_0$ when its amplitude is zero. Thereafter, it grows again, at the expense of the other components. The timescale for the exchange is $1/\gamma$. This is an exceptional solution of (9): it represents an isolated energy exchange, whereas all other solutions have periodic interplay between the modes.

The triad solutions are based on an assumption of small amplitudes, so that the effects of nonlinearity act like perturbations of a predominantly linear wave evolution. For larger amplitudes, further components are generated by nonlinear interactions, which enables a flux of energy to the largest scales. The very nature of the flow changes completely as the energy increases: mathematically, the equations are no longer integrable and physically the motion is no longer regular but becomes chaotic.

The conservation of energy and potential enstrophy are properties not only of resonant triads, but of the solutions of the complete equation (1) and, indeed, of its three-dimensional generalization, Charney's equation (3). The consequences for the energy spectrum of these constraints were investigated by Fjørtoft (1953) in the context of a nonrotating, nondivergent barotropic fluid. He showed that if a fraction of the energy flows into smaller scales, then a greater fraction must flow into larger scales. Platzman (1962) investigated the analytical dynamics of the spectral vorticity equation for nondivergent motions on the sphere. He showed that, with three components, concurrent energy changes in the components of smallest and largest scale are of the same sign, and opposite in sign to that of the component of intermediate scale. He pointed out that this "spectral blocking" is a direct consequence of the ex-

istence of two spectral invariants. Following the work of Kraichnan (1967), Fjørtoft's results were greatly extended by Charney (1971), in a paper titled *Geostrophic Turbulence.* Charney showed that an energy cascade to small scales was also precluded for three-dimensional quasigeostrophic flow, and he deduced a k^{-3} power law for the energy spectrum.

Let us consider an initial distribution of energy concentrated near a wavenumber K_0. As the flow evolves, the energy spectrum of the motion will broaden. But the enstrophy constraint requires that the mean wavenumber of the spectrum and the mean frequency must decrease. In other words, the spatial and temporal scales of the motion must *increase* with time. At the same time, the enstrophy is transferred to smaller scales. This is in marked contrast to the character of fully three-dimensional turbulence, where the energy cascades to smaller scales until frictional mechanisms begin to act. Richardson's (1922, p. 66) famous rhyme, "Big whirls have little whirls that feed on their velocity / And little whirls have lesser whirls and so on to viscosity," delightfully encapsulates the essence of the energy cascade in three-dimensional turbulence, but it does not accurately reflect large-scale quasigeostrophic dynamics. Pedlosky has suggested an analogy more appropriate to these motions, "Geostrophic turbulence more closely resembles big fish eating little fish and thriving on the diet" (Pedlosky 1987, p.174).[3]

NUMERICAL EXAMPLE OF TRIAD RESONANCE. In this section, numerical solutions of the barotropic potential vorticity equation (1) will be presented. The initial conditions correspond to a superposition of three Rossby wave components satisfying the conditions for resonance. We shall see that the solutions display the characteristics of a resonant triad, with a periodic interchange of energy between the modes. We first note an important property of the three-wave equations (9); if the amplitudes are scaled by a constant $\gamma$and the time is contracted by a similar factor, the form of the equations is unchanged. Thus, if $A(t) = [A_1(t),A_2(t),A_3(t)]$ is a solution of (9), then so is $\gamma A(\gamma t)$, for example, see (11). We conclude that the period of the modulation envelop will vary inversely with its amplitude. However, this scaling property will be inherited by the full equation (1) only as long as the modulation equations faithfully reflect the envelope dynamics of the full solution. This is the case as long as the perturbation procedure is valid, and this in turn requires that the nonlinear term in (1) is relatively small compared to the other terms. So, the scale invariance should be observed for small-amplitude waves, but may be expected to break down for larger-sized waves.

The parameters chosen for the numerical experiments have the following values: earth's radius is $a = 4 \times 10^7/2\pi$ m, domain size is $L_x = a$, $L_y = \frac{1}{3}a$, grid resolution is $N_x = 61$, $N_y = 21$, mean depth is $H_0 = 10$ km, acceleration of gravity is $g = \pi^2$ m s^{-2}, central latitude

TABLE S1. Parameters for resonant triad and initial conditions.

	Wave 1	Wave 2	Wave 3
Zonal wavenumber	–1	–3	4
Meridional wavenumber	–1	+1	0
k_n ($10^{-6}\times$)	–0.987	–2.961	3.948
ℓ_n ($10^{-6}\times$)	–3.109	3.109	0
$K_n^2 = k_n^2 + \ell_n^2$ ($10^{-11}\times$)	1.064	1.843	1.559
B_n ($10^{-23}\times$)	–1.746	–3.036	4.782
$\mu_n = (\lvert B_n\rvert \kappa_n^2)^{1/2}$($10^{-6}\times$)	1.275	1.280	1.746
Propagation (continuous):			
Frequency, σ_n ($10^{-6}\times$)	1.484	2.580	–4.064
Phase speed, c_n (m s^{-1})	–1.503	–0.871	–1.029
Period, τ (days)	49.01	28.18	17.89
Propagation (discrete):			
Frequency, σ_n ($10^{-6}\times$)	1.492	2.564	–4.026
Phase speed, c_n (m s^{-1})	–1.512	–0.866	–1.020
Period, τ (days)	48.73	28.36	18.06
Initial Conditions:			
Amplitude, $\lvert a_n\rvert$ (m)	0.095	0.055	0.409
Phase, ϕ_n	0	0	$\pi/2$

[3] Pedlosky's analogy has inspired the following ditty, of doubtful poetic merit, "Small whirls degenerate, down to the scale of quarks. / Big whirls swarm up, like fish into the jaws of sharks."

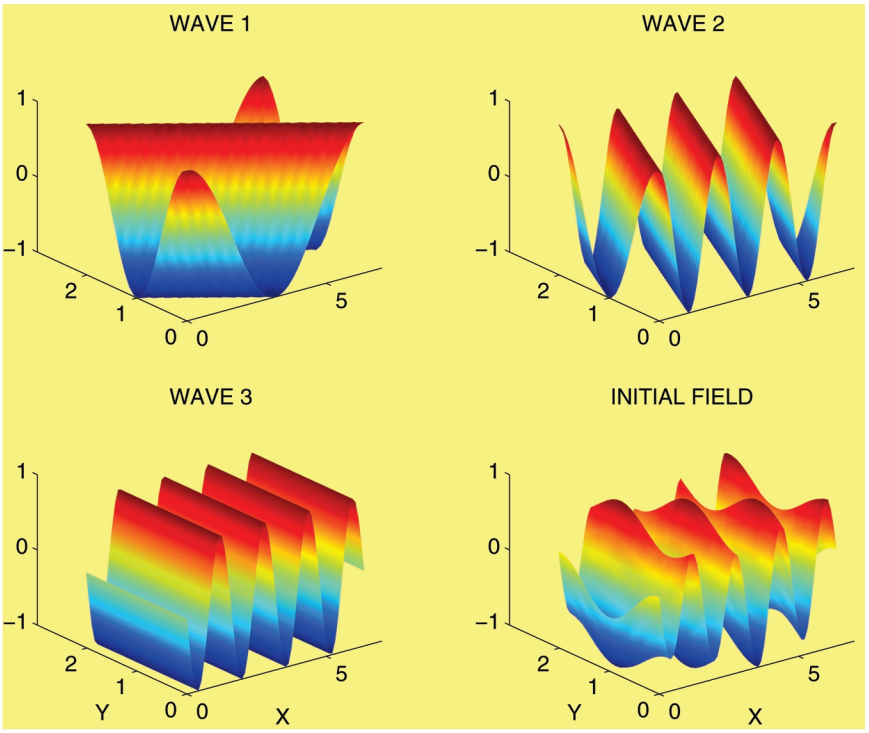

FIG. S2. Components of a resonant Rossby wave triad and the initial field constructed from them. All fields are scaled to have unit amplitude.

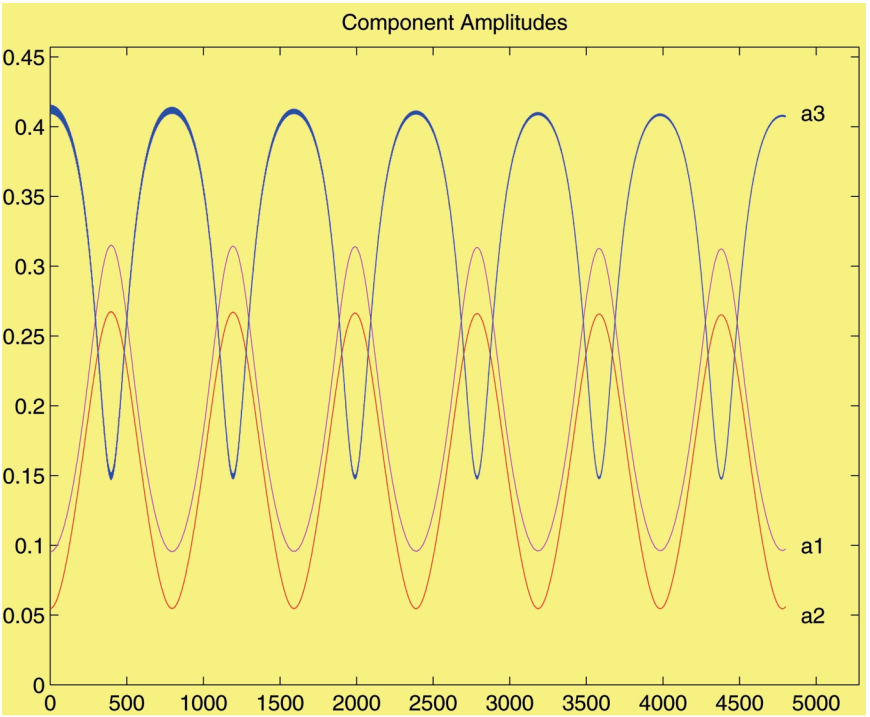

FIG. S3. Variation with time (days) of the amplitudes of the three components of the streamfunction. (The thickness of the a_3 line is due to high-frequency noise in the integration, which is gradually damped out by a weak Robert–Asselin filter.)

is $\phi_0 = 45°$, and rotation rate is $\Omega = 2\pi$ rad day^{-1}. Thus, we get a coriolis parameter $f_0 \approx 10^{-4}$ s^{-1}, beta parameter $\beta \approx 1.6 \times 10^{-11}$ m^{-1} s^{-1}, Rossby radius $L_R \approx 3 \times 10^6$ m, and parameter $F \approx 10^{-13}$ m^{-2} in (1). The means of defining the wavenumbers K_n and frequencies σ_n so that the conditions for resonance obtain are discussed in Pedlosky (1987). We shall not consider the details, but simply set down an example. The wavenumbers $(k_n \ell_n)$ of the three components are given in Table 1. Also given there are the frequencies, phase speeds, and periods of the components calculated using (2), and the corresponding values taking account of the effects of spatial discretization. The third component, that having the highest frequency, has a purely zonal variation ($\ell = 0$). It also has a spatial scale between that of the other components: $K_1 < K_3 < K_2$. It is easily shown that the conditions for resonance hold good for the triad

$$k_1 + k_2 + k_3 = 0,$$
$$\ell_1 + \ell_2 + \ell_3 = 0,$$
$$\sigma_1 + \sigma_2 + \sigma_3 = 0.$$

The three-wave components are plotted in Fig. S2 together with the initial streamfunction, which is a linear combination of them. For illustration, the waves are scaled to have unit amplitude; the actual amplitudes of the components are given in Table S1 (we give the amplitude of the geopotential height $h = f\psi/g$, which is measured in more ergonomic units than the streamfunction). We refer to wave 3 as the *primary component,* because it predominates at the initial time, and to the other components as secondary waves.

Equation (1) is solved by an elementary numerical technique;

the quantity $Q = [\nabla^2\psi - F\psi]$ is stepped forward using a leapfrog scheme, and the streamfunction is deduced by solving a Helmholtz equation with periodic boundary conditions at each time step. The Jacobian term is discretized following Arakawa (1966), so that the numerical scheme conserves both energy and enstrophy. [The MATLAB code for the solution of (1) is available online; see the "Summary and Discussion" section].

To illustrate resonance in its pure form, we choose the amplitude to be very small. According to the discussion above, this implies a very long interaction time. We show in Fig. S3 the evolution of the coefficients of the three components, obtained by applying an FFT (fast Fourier transform) to the ψ field at each time step. The thickness of the a_3 line is due to high-frequency noise in the integration, which is gradually damped out by a weak Robert–Asselin filter (Durran 1999). The periodic exchange of energy between the components is clear. Waves 1 and 2 grow and decay together, in antiphase with the third or primary wave. The modulation period is about 800 days,[4] with six cycles over the T = 4800-day duration of the integration.

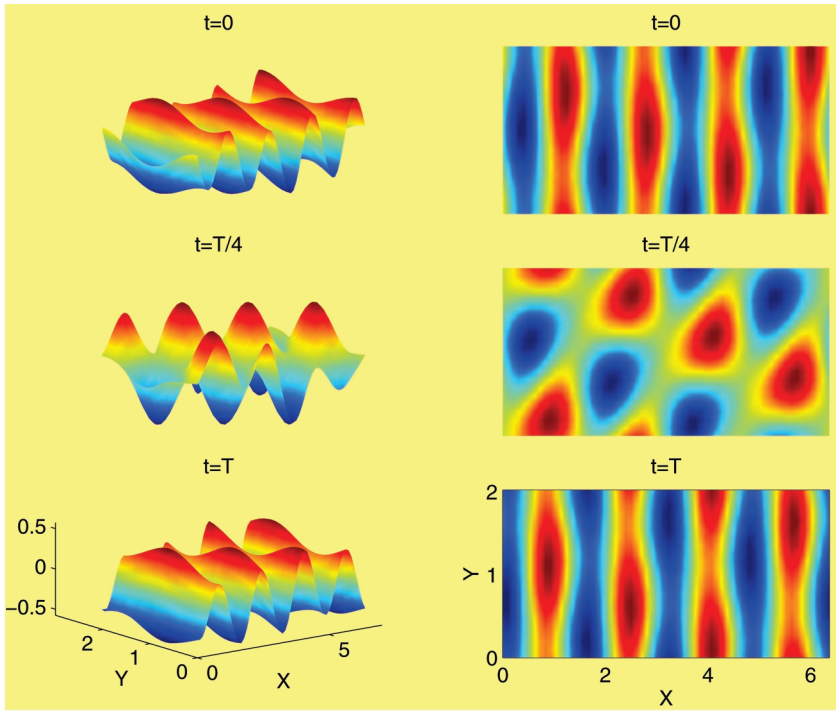

FIG. S4. Streamfunction at 3 times during an integration of duration T = 4800 days. Left-hand panels show perspective view and right-hand panels show a plan view.

In Fig. S4, we see the streamfunction valid at three different times. At $t = 0$ the streamfunction is dominated by the primary component, wave 3. At $t = T$, the solution looks very similar to that at the initial time (allowing for phase shifts due to the wave motion). The system has gone through six full cycles at this time. At $t = \frac{1}{4}T$, there is clearly a substantial contribution from the other waves, consistent with the values of the coefficients at this time (see Fig. S3). We remark here that while the amplitudes are clearly periodic, the phases need not return to their original values at the end of each modulation cycle.

THE SWINGING SPRING. The elastic pendulum or swinging spring is a simple mechanical system with highly complex dynamics. It comprises a heavy mass suspended from a fixed point by a light spring, which can stretch but not bend, moving under gravity. The equations of motion are easy to write down but, in general, impossible to solve analytically. For finite amplitudes, the motion of the system exhibits *chaos,* and predictability is severely limited. For small amplitudes, perturbation techniques are valid, the system is integrable, and approximate analytical solutions can be found.

The linear normal modes of the system are of two distinct types, a vertical or springing oscillation in which elasticity is the restoring force, and quasi-horizontal swinging oscillations in which the system acts like a pendulum. When the frequencies of the springing and swinging modes are in the ratio 2:1, an interesting nonlinear resonance phenomenon occurs, in which energy is transferred periodically back and forth between the springing and swinging motions. The resonance phenomenon was first examined by Vitt and Gorelik (1933), who were inspired by the analogy between this system and Fermi resonance of a carbon dioxide molecule.

Lynch (2002b) considered the swinging spring as a simple model of balance in the atmosphere, assuming the frequency of the elastic oscillations to be much greater than that of the pendular motions. He drew

[4] Choosing a more realistic amplitude drastically reduces the modulation period, as seen in the section titled "Precession and Predictability of Triads."

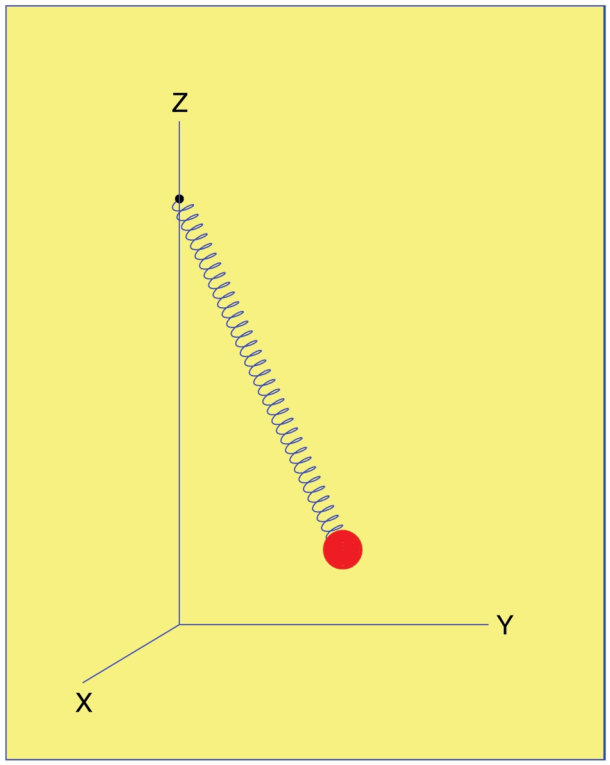

FIG. S5. The swinging spring: Cartesian coordinates are used, with the origin at the point of stable equilibrium of the bob. The pivot is at point (0, 0, ℓ).

an analogy between the elastic and pendular modes of the spring and the gravity and Rossby modes of oscillation in the atmosphere. He showed that the dynamics of several phenomena could be illustrated by the system, for example, the nonlinear interplay between low-frequency Rossby waves and high-frequency gravity waves, normal mode initialization of data to prevent spurious oscillations, filtering of the equations to eliminate the high-frequency solutions, existence and structure of a slow manifold, and onset of chaos. There are numerous references in Lynch (2002b) to earlier work on the elastic pendulum.

In Lynch (2002a), the resonance of the spring was studied. Asymptotic solutions were obtained, and an expression was derived for the precession of the swing plane. This was later generalized by Holm and Lynch (2002) who used Hamiltonian reduction and pattern evocation techniques to derive a formula for the stepwise precession of the azimuthal angle. Holm and Lynch discovered that the perturbation equations describing the motion of the swinging spring could be reduced to the three-wave equations; this is the *key result* leading to the present work. The relevance of the three-wave equations in a broad range of physical contexts was discussed by these authors.

EQUATIONS OF THE SPRING. The mechanical system is illustrated schematically in Fig. S5. We assume an unstretched spring length ℓ_0, length ℓ at equilibrium, spring constant k, and unit mass $m = 1$. The Lagrangian, approximated to cubic order in the amplitudes, is

$$L = \frac{1}{2}\left(\dot{x}^2 + \dot{y}^2 + \dot{z}^2\right) - \frac{1}{2}\left[\omega_R^2\left(x^2 + y^2\right) + \omega_Z^2 z^2\right] + \frac{1}{2}\lambda\left(x^2 + y^2\right)z, \tag{12}$$

where x, y, and z are Cartesian coordinates centered at the point of equilibrium; $\omega_R = (g/\ell)^{1/2}$ is the frequency of linear pendular motion; $\omega_Z = (k/m)^{1/2}$ is the frequency of its elastic oscillations; and $\lambda = \ell_0\omega_Z^2/\ell^2$. The Euler–Lagrange equations of motion may be written

$$\begin{aligned} \ddot{x} + \omega_R^2 x &= \lambda xz, \\ \ddot{y} + \omega_R^2 y &= \lambda yz, \\ \ddot{z} + \omega_Z^2 z &= \frac{1}{2}\lambda\left(x^2 + y^2\right). \end{aligned} \tag{13}$$

If we assume that the amplitude of the motion is small, we can ignore the right-hand terms, and the solutions may be written in the form of pure sinusoidal oscillations. In this linear limit, there is no interaction between the oscillations in each direction. It is easily shown that the rotational frequency is always less than the elastic, $|\omega_R| < |\omega_Z|$.

In general, there are two constants of the motion for (13), the energy $E = T + V$ and the angular momentum $j = m(x\dot{y} - y\dot{x})$ about the vertical. Because the system has 3 degrees of freedom and only two invariants, it is not integrable. We must employ perturbation techniques to obtain an approximate solution. We confine attention to the resonant case $\omega_Z = 2\omega_R$ and apply the averaged Lagrangian technique (see, Holm and Lynch 2002, for details). The solution of (13) is assumed to be of the form

$$\begin{aligned} x &= \Re[a(t)\exp(i\omega_R t)], \\ y &= \Re[b(t)\exp(i\omega_R t)], \\ z &= \Re[c(t)\exp(2i\omega_R t)]. \end{aligned} \tag{14}$$

The coefficients $a(t)$, $b(t)$, and $c(t)$ are assumed to vary on a timescale, which is much longer than the timescale of the oscillations $\tau = 2\pi/\omega_R$. If the Lagrangian

is averaged over time τ, the Euler–Lagrange equations for the modulation amplitudes are

$$\begin{aligned} i\dot{a} &= \kappa a^* c, \\ i\dot{b} &= \kappa b^* c, \\ i\dot{c} &= \frac{1}{4}\kappa\left(a^2 + b^2\right), \end{aligned} \tag{15}$$

where $\kappa = \lambda/(4\omega_R)$. These are the complex versions of Eqs. (68)–(73) in Lynch (2002a), which were derived using the method of multiple timescale analysis. If we now introduce new dependent variables A_1, A_2, and A_3 defined by

$$\begin{aligned} A_1 &= \frac{1}{2}\kappa(a + ib), \\ A_2 &= \frac{1}{2}\kappa(a - ib), \\ A_3 &= i\kappa c, \end{aligned} \tag{16}$$

the equations of motion take the following form:

$$\begin{aligned} \dot{A}_1 &= -A_2^* A_3, \\ \dot{A}_2 &= -A_3 A_1^*, \\ \dot{A}_3 &= +A_1 A_2. \end{aligned} \tag{17}$$

Thus, the modulation equations for the swinging spring are transformed into the *three-wave equations,* mathematically identical to the equations (9) previously obtained for resonant Rossby triads.

The three-wave equations conserve the following three quantities,

$$H = \left(A_1 A_2 A_3^* - A_1^* A_2^* A_3\right)/2i, \tag{18}$$

$$N = |A_1|^2 + |A_2|^2 + 2|A_3|^2, \tag{19}$$

$$J = |A_1|^2 - |A_2|^2. \tag{20}$$

The first, $H = \Im\{A_1 A_2 A_3^*\}$, is the Hamiltonian of the system (see Holm and Lynch 2002). The second, *N,* is a measure of the energy of the oscillations and the third, *J,* is the angular momentum. The following positive definite combinations of *N* and *J* are significant:

$$\begin{aligned} N_1 &\equiv \frac{1}{2}(N + J) = |A_1|^2 + |A_3|^2, \\ N_2 &\equiv \frac{1}{2}(N - J) = |A_2|^2 + |A_3|^2. \end{aligned}$$

These are the Manley–Rowe relations introduced above, which are discussed in the extensive literature on three-wave interactions. The quantities *H, N*$_1$, and *N*$_2$ provide three independent constants of the motion.

The three-wave equations model the nonlinear dynamics of the amplitudes of three waves in fluids or plasmas. Resonant wave–triad interactions play an essential role in the generation of turbulence and in determining the statistics of the power spectrum. We have seen that energy and enstrophy are conserved for a Rossby wave triad. These quantities may easily be combined to produce the Manley–Rowe quantities. Equations (17) are also equivalent to the Maxwell–Schrödinger envelope equations for the interaction between radiation and a two-level resonant medium in a microwave cavity. The three-wave system also describes the dynamics of the envelopes of light waves interacting quadratically in nonlinear material, and of triplets of phonons, vibrations in crystal lattices. Using a geometrical approach, the reduced dynamics for the wave intensities may be represented as motion on a closed surface in three dimensions—the three-wave surface (see Holm and Lynch 2002, for a fuller discussion of the three-wave system and for further references).

For the special case where the Hamiltonian takes the value zero, the system (17) reduces to three *real* equations for $X = |A_1|$, $Y = |A_2|$, and $Z = |A_3|$:

$$\dot{X} = -YZ, \quad \dot{Y} = -ZX, \quad \dot{Z} = +XY. \tag{21}$$

There are three equilibrium solutions when two components of (*X, Y, Z*) vanish. Two are stable (conical rotation of the spring without stretching, clockwise or anticlockwise) and one is unstable (vertical oscillation). Equation (21) is equivalent to Euler's equations for the rotation of a free rigid body rotating about its center of gravity (Synge and Griffith 1959). We recall that Euler's equations are

$$\begin{aligned} I_1\dot{\Omega}_1 &= \left(I_2 - I_3\right)\Omega_2\Omega_3, \\ I_2\dot{\Omega}_2 &= \left(I_3 - I_1\right)\Omega_3\Omega_1, \\ I_3\dot{\Omega}_3 &= \left(I_1 - I_2\right)\Omega_1\Omega_2, \end{aligned} \tag{22}$$

where $I_1 < I_2 < I_3$ are the moments of inertia and Ω_j are the angular velocity components. Two of the right-hand coefficients are negative and one is positive. Equation (22) is easily converted to the form (21) by rescaling the dependent variables. There are three equilibrium solutions, when two of the angular velocity components vanish. It is well known that rotation about the I_2 axis is unstable, whereas rotation about the remaining principal axes is stable. This is easily demonstrated by twirling a book (bound with an elastic band): it will spin smoothly about the top-to-bottom axis and the front-to-back axis, but topple irregularly about the axis through the spine, which has the moment of inertia with intermediate value. Energy and total angular momentum,

$$E = \frac{1}{2}\left(I_1\Omega_1^2 + I_2\Omega_2^2 + I_3\Omega_3^2\right),$$
$$L^2 = \frac{1}{2}\left(I_1^2\Omega_1^2 + I_2^2\Omega_2^2 + I_3^2\Omega_3^2\right),$$

are the physically significant conserved quantities for the rigid body. Their formal similarity to the energy and enstrophy of a Rossby triad, (6) and (7), is immediate. Thus, the simple spring pendulum, which was first studied to provide a classical analog to the quantum phenomenon of Fermi resonance, provides a concrete mechanical system that simulates a wide range of physical phenomena, in particular the phenomenon of interest here, the resonance of Rossby wave triads.

PRECESSION OF THE SWING PLANE. There is a particular feature of the behavior of the physical spring, which is fascinating to watch. When started with almost vertical springing motion, the movement gradually develops into an essentially horizontal swinging motion. This does not persist, but is soon replaced by springy oscillations similar to the initial motion. Again, a horizontal swing develops, but now in a different direction. This variation between springy and swingy motion continues indefinitely. The change in direction of the swing plane from one horizontal excursion to the next is difficult to predict; the plane of swing precesses in a manner that is quite sensitive to the initial conditions. Lynch (2002a) derived an expression for the angle of precession, and Holm and Lynch showed that it was a particular case of a more general family of expressions:

$$\Omega = -\frac{2\kappa\Im\{abc^*\}}{|a|^2 - |b|^2}. \tag{23}$$

Here, $\Omega(t)$ is the rate of rotation of the swing plane and the precession angle Θ can be ascertained by integrating over the time interval of the motion: $\Theta = \int_0^t \Omega(t')dt'$. In the special case where a and b are 90° out of phase, one finds by using the constants of motion that

$$\Omega = \frac{2\kappa JH}{\left(N - 4|c|^2\right)^2 - 4J^2}. \tag{24}$$

In this special case, Ω can be computed as soon as $|c|$ is known.[5]

NUMERICAL EXAMPLE OF SPRING PRECESSION. To illustrate the nature of the modulated motion, we present the results of some numerical integrations of the spring equations (13). The parameter values are $m = 1$ kg, $\ell = 1$ m, g = π^2 m s^{-2}, and $k = 4\pi^2$ kg s^{-2}, so that $\omega_R = \pi$ and $\omega_Z = 2\pi$. The linear swinging mode has period $\tau_R = 2$ s, and the springing mode has half this period, $\tau_Z = 1$ s. The initial conditions are set as follows:

$$\begin{aligned}\left(x_0, y_0, z_0\right) &= (0.04, 0, 0.08),\\ \left(\dot{x}_0, \dot{y}_0, \dot{z}_0\right) &= (0, 0.03427, 0).\end{aligned} \tag{25}$$

The corresponding initial values for the modulation equations (15) are given by

$$\begin{aligned}a_0 &= x_0 + \dot{x}_0/i\omega_R,\\ b_0 &= y_0 + \dot{y}_0/i\omega_R,\\ c_0 &= z_0 + \dot{z}_0/i\omega_Z.\end{aligned} \tag{26}$$

In Fig. S6 we plot the solutions *x, y,* and *z* obtained by integrating (13) from the initial conditions (25). Also plotted (lower-right-hand panel) are the components of energy, showing the periodic exchange between the horizontal and vertical components. During the integration time of 150 s there are six horizontal excursions, so the modulation period is about 25 s.

The stepwise precession of the swinging spring will now be illustrated. In Holm and Lynch (2002) the

[5] A Java Applet illustrating the precession of the swinging spring may be found online at http://www.maths.tcd.ie/~plynch/SwingingSpring/SS_Home_Page.html.

concept of an *instantaneous ellipse* was introduced: at any time, the spring trajectory can be approximated by a central ellipse, and the rotation of its major axis represents the precession of the amplitude envelope. In Fig. S7 (top panel), we plot the azimuthal angle θ (in degrees) and magnitude of the major axis of the ellipse (scaled to have a maximum value of 180). The stepwise precession is clearly seen. In the bottom panel, we plot the horizontal projection, y vs x, and obtain a star-shaped pattern. The precession angle between horizontal excursions is 30° (the value of y_0 was tweaked to tune the precession angle to an even fraction of 360°). Thus, the major axis passes through 180° in 150 s.

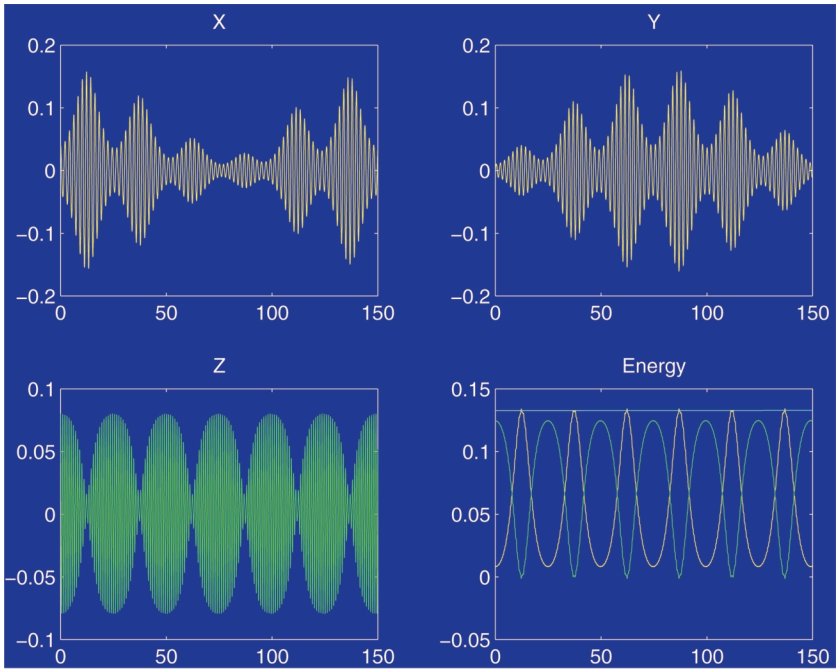

FIG. S6. Solutions *x*, *y*, and *z* obtained by integrating (13) (for initial conditions, see text). Also plotted (lower-right-hand panel) are the components of energy (yellow: horizontal; green: vertical; cyan: total).

PRECESSION AND PREDICTABILITY OF TRIADS. Analogies between physical systems are a powerful means of gaining understanding of abstruse and complex phenomena from more familiar and simple systems. When the equations describing the systems are identical, more concrete conclusions can be reached. Because the same equations apply to both the spring and triad systems, the stepwise precession of the spring must have a counterpart for triad interactions. Expressions for the axes and azimuth of the instantaneous ellipse in terms of the amplitudes, *a*, *b*, and *c* of the spring were given in Holm and Lynch (2002). In terms of the variables of the three-wave equations, they are even simpler. The semiaxes and azimuthal angle θ are given by

$$\begin{aligned} A_{\mathrm{maj}} &= |A_1| + |A_2|, \\ A_{\mathrm{min}} &= |A_1| - |A_2|, \\ \theta &= \frac{1}{2}(\varphi_1 - \varphi_2). \end{aligned} \tag{27}$$

The area of the ellipse is $\pi A_{\mathrm{maj}} A_{\mathrm{min}} = \pi J$, constant (we have ignored an unimportant factor κ in the semiaxes). The initial conditions (25) for the spring, which were used to generate the solution shown in Fig. S7, were transformed by means of (26), (16), (8), and (4), to obtain corresponding initial conditions for (1). The initial field was then scaled to ensure that the small-amplitude approximation was accurate (the amplitude of the primary component was set to 0.4 m).

The coefficients of the components were saved and the elements of the instantaneous ellipse were calculated using (27). The time variation of θ is similar to that found for the spring (cf. Figs. S7 and S8) exhibiting a characteristic stepwise precession. Figure S8 (bottom panel) shows a polar plot of A_{maj} versus θ. We immediately see the starlike pattern, similar to that found for the spring (Fig. S7). The precession angle, the change in azimuth between successive maxima of A_{maj}, is again about 30°. This is remarkable, and illustrates the value of the analogy; phase precession for Rossby wave triads has not been noted before, and is an example of the insight coming from the mathematical equivalence of the two systems.

The initial amplitudes resulting directly from (25) were huge. To obtain small amplitudes (wave 3 having amplitude 0.4 m) a scaling factor $\gamma = 3.4 \times 10^{-7}$ was applied. The modulation period of 25 s for the spring should increase by $1/\gamma$, giving a value of 850 days. The period observed for the modulation of the triad is about 800 days, in reasonable agreement with this broad scaling argument. We note that while the precession rate Ω in (23) scales as γ, the precession

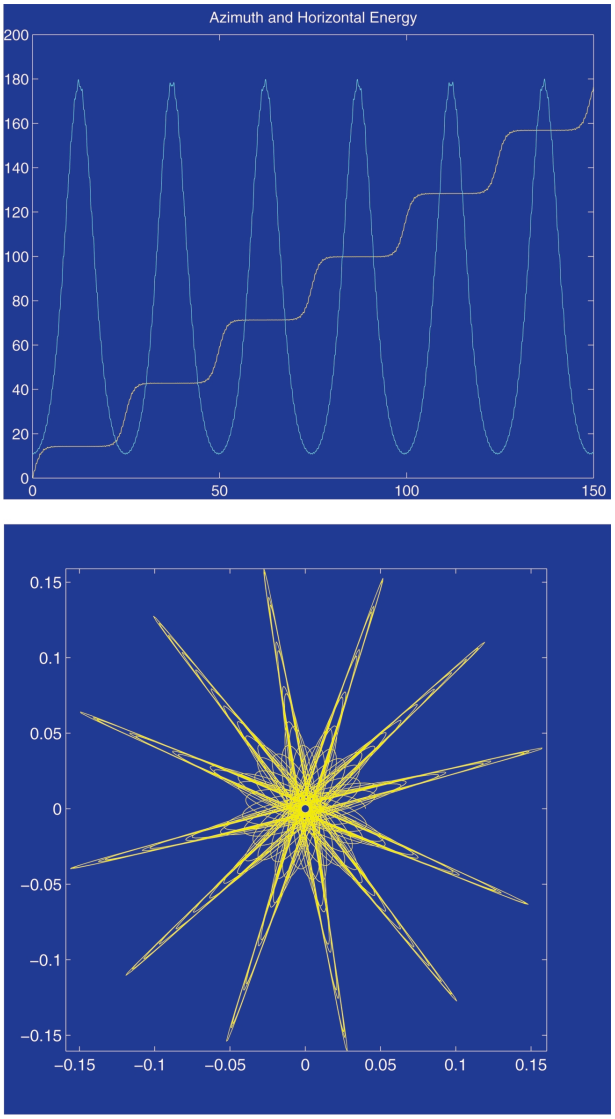

FIG. S7. (top) Azimuth θ (yellow) and horizontal energy (cyan) of spring solution. (bottom) Horizontal projection of spring solution, y vs x. The precession angle between horizontal excursions is 30° and the major axis passes through 180° in 150 s.

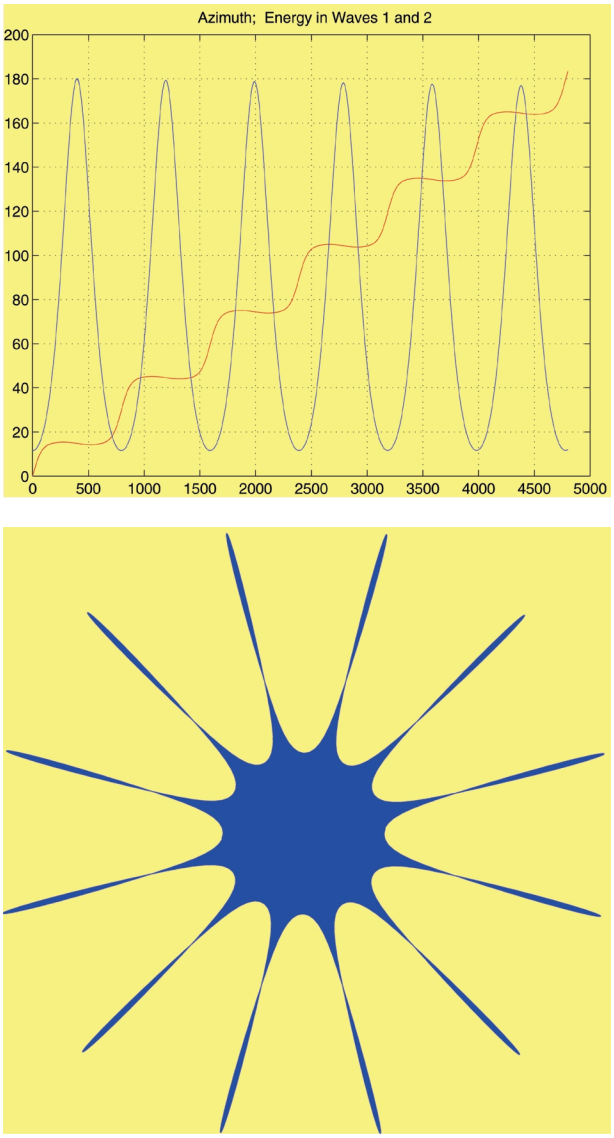

FIG. S8. (top) Azimuth θ of instantaneous ellipse (see text) and energy of waves 1 and 2. (bottom) Polar plot of A_{maj} vs θ. The starlike pattern is similar to that found for the spring (Fig. S7). The precession angle is again about 30°.

angle Θ is independent of scale. Indeed, we find that the precession angle is approximately 30° for both spring and triad.

The precession has implications for the predictability of atmospheric motion. A flow dominated by a single Rossby wave may be unstable and, if so, will be rapidly distorted due to inevitable perturbations. Triad resonance is the primary mechanism for this breakdown. However, the resulting pattern is highly sensitive to details of minute perturbations, which are impossible to determine accurately. Let us assume an initial state dominated by the primary wave ($|A_1| \ll |A_3|$ and $|A_2| \ll |A_3|$). We note a symmetry of the three-wave equations (9); if the variables are transformed by

$$A_1' = A_1 \exp(i\chi_1),$$

$$A_2' = A_2 \exp(i\chi_2),$$

$$A_3' = A_3 \exp[i(\chi_1 + \chi_2)],$$

the equations remain unchanged. Clearly, $H = \Im\{A_1 A_2 A_3^*\}$ is invariant under this transformation. In particular, if the signs of the initial values $A_1(0)$ and $A_2(0)$ are both changed ($\chi_1 = \chi_2 = \pi$), we obtain a so-

lution $(A_1', A_2', A_3) = (-A_1, -A_2, A_3)$, identical to the original one but with the signs of these two components reversed. Thus, after half a modulation cycle, when A_1 and A_2 are no longer small, drastically different patterns can result from states that are initially very similar.

For purposes of illustration, we haven chosen small amplitudes for the examples so far. If the initial fields are scaled up by a factor γ', the timescale for the solutions to diverge is reduced by a similar factor. An important question is whether the sensitivity to initial conditions is found for realistic amplitudes of the waves. We consider now a primary wave of amplitude 60 m, and secondary waves of amplitude 0.6 m. This is a factor of 150 larger than the example shown in Fig. S3. Thus, according to the scaling properties of the three-wave equations discussed in the section titled "Numerical Example of Triad Resonance," the modulation half-cycle time should be reduced from 400 to about 2.7 days. We integrate over a period $T = 4$ days. Figure S9 shows the initial and final fields for two integrations of Eq. (1). The initial fields differ only in the sign of the perturbation. Considering the top panels of Fig. S9 as two weather "analyses," we would have to regard them as practically identical (the perturbation amplitude is only 1% of that of the primary wave). Yet, the resulting "forecasts," in the two bottom panels, differ drastically. The center point is marked by a yellow plus sign. In one case (lower-left-hand panel) it is close to a high pressure center (red); in the other (lower-right-hand panel) it is close to a low (blue). Thus, the forecasts from almost identical initial conditions diverge significantly within a matter of a few days.[6]

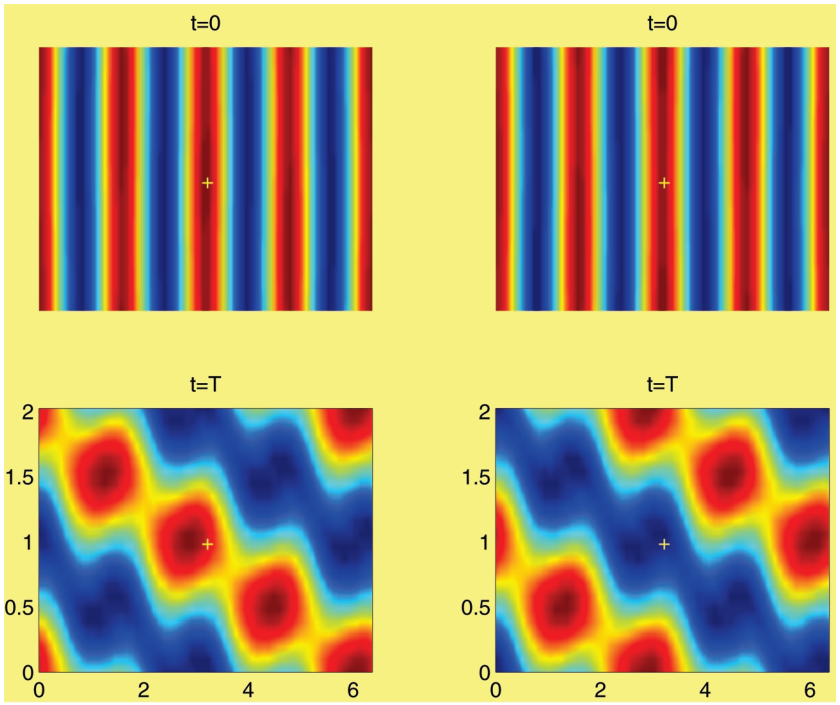

FIG. S9. Initial and final fields for two 4-day integrations of Eq. (1). The initial fields (top panels) differ only in the sign of the perturbation. The resulting forecasts are shown in the two bottom panels. The center of the domain is marked by a yellow cross.

Consider the three-wave equations (9) in the case $|A_1| \ll |A_3|$ and $|A_2| \ll |A_3|$:

$$\ddot{A}_1 \approx |A_3|^2 A_1,$$
$$\ddot{A}_2 \approx |A_3|^2 A_2,$$
$$\dot{A}_3 \approx 0.$$

Thus, A_3 is effectively constant and both A_1 and A_2 grow exponentially. Of course, this growth does not continue indefinitely. Nevertheless, two close but differing states with $|A_{1,2}| \ll |A_3|$ will diverge rapidly so that there is exponential sensitivity to initial conditions. Because the three-wave equations are integrable, this sensitivity cannot be described in the usual terms of chaos (the solutions of these equations are regular). We, therefore, have a chaoslike phenomenon in an integrable system. This is precisely what we have seen in Fig. S9. The implication is that predictability may be severely limited even in systems that are not chaotic (i.e., that do not have positive Lyapunov exponents, defined as long time limits).

The task of forecasting Rossby wave breakdown may be compared to that of trying to predict the emergence of a growing perturbation in a baroclinically unstable flow. Because the location of the perturbation is unknown, the phase of the developing baroclinic wave cannot be anticipated before it has grown to a detectable amplitude. In the case of the

[6] The 4-day period chosen for this example is arbitrary; the interaction time is sensitive to changes in the amplitude of the triad components, that is, to the chosen scaling factor.

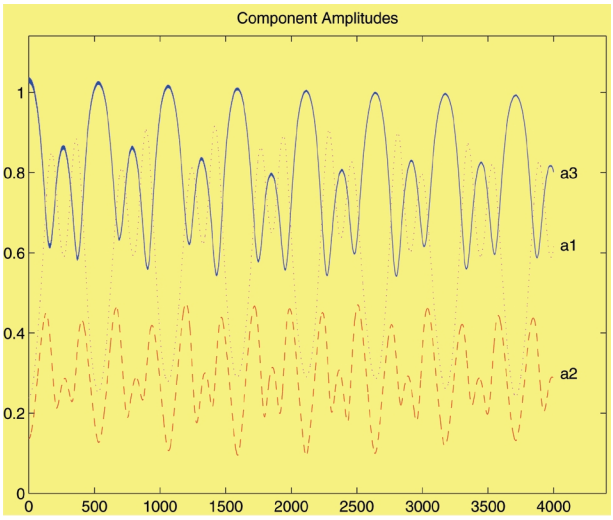

FIG. S10. Evolution of the coefficients of the three components for initial conditions scaled by 2.5 relative to those in Fig. S3. The period exchange of energy between the components indicates a period-doubling route to chaos.

unstable Rossby wave, although accurate knowledge of the primary wave phase is available, it is of no help in estimating the phases of the growing perturbations, which soon dominate the flow. The forecaster's task is even harder than might have been imagined.

For realistic Rossby waves, the small-amplitude approximation is invalid, and we would expect the flow to become chaotic. The nature of the transition from the integrable solutions of the three-wave equations to irregular chaotic flow is worthy of attention. We do not undertake a detailed study but show a single example in Fig. S10. The component amplitudes are scaled by 2.5 relative to those upon which Fig. S3 is based. But now something interesting happens: large and small peaks alternate, suggesting that the period for energy exchange between the wave components has doubled. This period-doubling bifurcation is a well-known path to chaos (Ott 1993), and this preliminary evidence should encourage a more detailed investigation to confirm if the period-doubling mechanism is at work here.

SUMMARY AND DISCUSSION. We have considered the interactions between resonant triads of Rossby waves, by integrating the barotropic potential vorticity equation (1) from appropriately chosen initial conditions. The behavior for small amplitude is consistent with that predicted by a perturbation analysis; the total energy of the triad is constant, but the energy is exchanged on a slow timescale between the components. The perturbation analysis leads to the three-wave equations, an integrable system. These same equations govern the small-amplitude dynamics of an elastic pendulum or swinging spring. This equivalence allows us to deduce properties, not otherwise evident, of atmospheric flow from the behavior of the mechanical system. In particular, we have seen that the stepwise precession found for the spring is also a characteristic of triad interactions.

When a single wave, the primary wave, dominates the initial conditions, the subsequent development is found to depend sensitively on the details of the perturbation. Because, in general, these details are unobservable, accurate prediction of the flow is difficult or impossible.[7] The question of the extent to which these findings apply to more complex situations, such as atmospheric flow, depends on how spherical and baroclinic effects influence the dynamics. For flow on the sphere, a single large-scale Rossby wave may be stable, because it may not be possible to find a resonant triad such that the scale of this primary wave is intermediate between those of the other two components. Evidence from elsewhere suggests that the largest-scale Rossby waves are indeed stable (Lorenz 1972; Hoskins 1973).

The MATLAB code for solving the barotropic potential vorticity equation is available online at www.maths.tcd.ie/~plynch/Rossby_Wave_Triads/triad.html and the code to integrate the swinging spring equations may be found at www.maths.tcd.ie/~plynch/Rossby_Wave_Triads/spring.html. These programs may be used to pursue the study of the equivalence between the two systems. For example, two-dimensional planar motion of the spring corresponds to triad interactions for which the two secondary wave envelopes are locked in phase and proportional in amplitude. The elliptic–parabolic modes of the spring discussed by Lynch (2002a) must also have counterparts for triad dynamics. The transition to turbulence for triad motions merits a more detailed study.

Finally, we mention that the implications of the spring dynamics are much wider than discussed above. For example, drift waves in magnetic confinement devices, such as tokamaks, are believed to dominate the turbulent transport of energy. They are also relevant for the dynamics of the ionosphere and magnetosphere. The three-wave equations are central to the small-amplitude dynamics of all these systems.

[7] This situation corresponds to spring oscillations that are initially quasi-vertical; it is virtually impossible to predict the direction of the first horizontal excursion.

ACKNOWLEDGMENTS. I have benefitted enormously from conversations and correspondence with many friends and colleagues. In particular, I should like to thank Prof. George Platzman for his enlightening comments on the paper. In addition, I am grateful to Silvia Annibaldi, Ray Bates, Gerard Cats, Tony Hollingsworth, Brian Hoskins, Jim Logue, Aidan McDonald, Tim Palmer, Joe Pedlosky, Anders Persson, Norman Phillips, and Adrian Simmons for helpful discussions and comments. My thanks to Phil Morrison (Austin) who first drew my attention to the resonance phenomenon for the swinging spring, to Rick Salmon (Scripps) who suggested using the averaged Lagrangian technique to analyze its motion, and especially to Darryl Holm (Los Alamos) for fruitful and enjoyable collaboration in which the three-wave equations linking the spring with the atmosphere emerged.

REFERENCES

Arakawa, A., 1966: Computational design for long-term numerical integration of the equations of fluid motion: Two-dimensional incompressible flow, Part I. *J. Comput. Phys.,* **1,** 119–143.

Bretherton, F. P., 1964: Resonant interactions between waves. The case of discrete oscillations. *J. Fluid Mech.,* **20,** 457–479.

Cartwright, D. E., 1999: *Tides: A Scientific History.* Cambridge University Press, 292 pp.

Charney, J. G., 1948: On the scale of atmospheric motions. *Geofys. Publ.,* **17,** 3–17.

——, 1971: Geostrophic turbulence. *J. Atmos. Sci.,* **28,** 1087–1095.

——, 1973: Planetary fluid dynamics. *Dynamic Meteorology,* E. P. Morel, Ed., D. Reidel, 97–351.

——, and M. E. Stern, 1962: On the stability of internal baroclinic jets in a rotating atmosphere. *J. Atmos. Sci.,* **19,** 159–172.

Durran, D. R., 1999: *Numerical Methods for Wave Equations in Geophysical Systems.* Springer-Verlag, 465 pp.

Fjørtoft, R., 1953: On the changes in the spectral distribution of kinetic energy for two-dimensional nondivergent flow. *Tellus,* **5,** 225–230.

Flattery, T. W., 1967: Hough Functions. Ph.D. dissertation, University of Chicago, 168 pp. [Also published as Dept. Geophysical Science, University of Chicago Tech. Rep. 21, 175 pp.]

Hasegawa, A., and K. Mima, 1977: Pseudo-three-dimensional turbulence in magnetized nonuniform plasmas. *Phys. Fluids,* **21,** 87–92.

Haurwitz, B., 1937: The oscillations of the atmosphere. *Gerlands Beit. Geophys.,* **51,** 195–233.

——, 1940a: The motion of atmospheric disturbances. *J. Mar. Res.,* **3,** 35–50.

——, 1940b: The motion of atmospheric disturbances on the spherical earth. *J. Mar. Res.,* **3,** 254–267.

Holm, D. D., and P. Lynch, 2002: Stepwise precession of the resonant swinging spring. *SIAM J. Appl. Dyn. Syst.,* **1,** 44–64.

Horton, W., and A. Hasegawa, 1994: Quasi-two-dimensional dynamics of plasmas and fluids. *Chaos,* **4,** 227–251.

Hoskins, B. J., 1973: Stability of the Rossby–Haurwitz wave. *Quart. J. Roy. Meteor. Soc.,* **99,** 723–745.

Hough, S. S., 1898: On the application of harmonic analysis to the dynamical theory of the tides. Part II: On the general integration of Laplace's dynamical equations. *Philos. Trans. Roy. Soc. London,* **191A,** 139–185.

Kasahara, A., 1976: Normal modes of ultralong waves in the atmosphere. *Mon. Wea. Rev.,* **104,** 669–690.

Kraichnan, R., 1967: Inertial ranges in two-dimensional turbulence. *Phys. Fluids,* **10,** 1417–1423.

Lamb, H., 1895: *Hydrodynamics.* 2d ed. Cambridge University Press, 342 pp.

Lewis, J. M., 1992: Carl-Gustaf Rossby: A study in mentorship. *Bull. Amer. Meteor. Soc.,* **73,** 1425–1438.

Lindzen, R. S., E. N. Lorenz, and G. W. Platzman, Eds., 1990: *The Atmosphere—A Challenge: The Science of Jule Gregory Charney.* Amer. Meteor. Soc., xviii + 321 pp.

Longuet-Higgins, M. S., 1968: The eigenfunctions of Laplace's tidal equations over a sphere. *Philos. Trans. Roy. Soc. London,* **262A,** 511–607.

Lorenz, E. N., 1972: Barotropic instability of Rossby wave motion. *J. Atmos. Sci.,* **29,** 258–264.

Lynch, P., 2002a: Resonant motions of the three-dimensional elastic pendulum. *Int. J. Nonlinear Mech.,* **37,** 345–367.

——, 2002b: The swinging spring: A simple model for atmospheric balance. *Geometric Methods and Models,* J. Norbury and I. Roulstone, Eds., Vol. 2, *Large-Scale Atmosphere–Ocean Dynamics,* Cambridge University Press, 64–108.

——, 2003: Resonant Rossby wave triads and the swinging spring. *Bull. Amer. Meteor. Soc.,* **84,** in press.

Margules, M., 1893: Luftbewegungen in einer rotierenden Sphäroidschale. *Sitzungsber. Kais. Akad. Wiss. Wien,* IIA, **102,** 11–56.

Nezlin, M. V., and E. N. Snezhkin, 1993: *Rossby Vortices, Spiral Structures, Solitons. Astrophysics and Plasma Physics in Shallow Water Experiments.* Springer-Verlag, 223 pp.

Obukhov, A. M., 1949: On the question of the geostrophic wind (in Russian). *Izv. Akad. Nauk. SSSR. Ser. Geogr. Geofiz.,* **13,** 281–306. (Translated by J. C. Howcroft, University of Chicago, 1962.)

Ott, E., 1993: *Chaos in Dynamical Systems.* Cambridge University Press, 385 pp.

Pedlosky, J., 1987: *Geophysical Fluid Dynamics.* 2d ed. Springer, 710 pp.

Phillips, N. A., 1990: The emergence of quasi-geostrophic theory. *The Atmosphere—A Challenge: The Science of Jule Gregory Charney,* R. S. Lindzen et al., Eds., Amer. Meteor. Soc., 177–206.

——, 1998: Carl-Gustaf Rossby: His times, personality, and actions. *Bull. Amer. Meteor. Soc.,* **79,** 1097–1112.

——, W. Blumen, and O. Coté, 1960: Numerical weather prediction in the Soviet Union. *Bull. Amer. Meteor. Soc.,* **41,** 599–617.

Platzman, G. W., 1962: The analytical dynamics of the spectral vorticity equation. *J. Atmos. Sci.,* **19,** 313–328.

——, 1968: The Rossby Wave. Symons Memorial Lecture, 3 April, 1968. *Quart. J. Roy. Meteor. Soc.,* **94,** 225–248.

——, 1985: Conversations with Bernhard Haurwitz. NCAR Tec. Note TN-257, 184 pp.

Richardson, L. F., 1922: *Weather Prediction by Numerical Process.* Cambridge University Press, xii + 236 pp. (Reprinted by Dover Publications, 1965, with a new Introduction by S. Chapman, xvi + 236 pp.)

Rossby, C. G., and Coauthors, 1939: Relations between variations in the intensity of the zonal circulation of the atmosphere and the displacements of the semi-permanent centers of action. *J. Mar. Res.,* **2,** 38–55.

Synge, J. L., and B. A. Griffith, 1959: *Principles of Mechanics.* McGraw-Hill, 552 pp.

Vitt, A., and G. Gorelik, 1933: Kolebaniya uprugogo mayatnika kak primer kolebaniy dvukh parametricheski svyazannykh linejnykh sistem. *Zh. Tekh. Fiz.,* **3,** 294–307. (Oscillations of an elastic pendulum as an example of the oscillations of two parametrically coupled linear systems. Translated by L. Shields, Met Éireann Historical Note No. 3, 15 pp.)